

# An Image Fusion Algorithm based on Nonsampled Contourlet Transform

<sup>1</sup>PAI ZHANG, <sup>1</sup>LIXIA WANG, <sup>2</sup>TAO HOU

<sup>1</sup>College of Intelligence and Information Engineering, Tangshan University, CHINA

<sup>2</sup>Beijing Aerospace Xinli Technology Co., Ltd, Beijing, CHINA

**Abstract**—In this paper, a multisensor image fusion method based on non-sampling Contourlet transform is proposed. The transform has translation invariance, is suitable for expressing images with rich detail information and direction information, and can avoid the ringing effect introduced by general methods to the fused images. The image is decomposed by the transform to obtain high and low frequency components. The high-frequency component uses PCNN as the fusion rule, and the low-frequency component uses the golden section method to search the optimal low-frequency fusion weight, so as to fuse the low-frequency subband coefficients of multi-sensor images adaptively. Comparative experimental results show that the proposed method can achieve better fusion effect.

**Keywords**—Nonsampled Contourlet transform, image fusion, PCNN, Golden section method

Received: March 8, 2021. Revised: March 21, 2022. Accepted: April 23, 2022. Published: May 18, 2022.

## 1. Introduction

Image fusion is a data fusion [1] based on image. It means that at the same time, simultaneous interpreting two or more than two images from different bands of the same scene or from different sensors, and forming a composite image to get more picture processing process on target information. Multi focus image fusion refers to the synthesis of two or more images with different focal lengths, filtering out the blurred parts of two or more images and retaining their clear parts, so as to better observe and analyze the image.

Image fusion technology is playing a more and more important role in modern aerospace, automatic control, remote sensing and telemetry, medicine, especially in the field of military command [2-5].

Image fusion methods can be divided into two categories. One is to directly perform weighted average processing on the matched source image in the spatial domain, so as to obtain a new fused image. This method is simple and easy to operate, but it ignores the simultaneous interpreting of different sensor images.

The difference in the amount of important information contained in the corresponding target area. The other is based on transform domain. These methods use multi-scale transformation as a tool to extract the salient features of images. Typical methods are wavelet based methods [6-9], and wavelet based image fusion methods can provide better image fusion performance [8].

Two dimensional separable wavelet transform is formed by one-dimensional wavelet through tensor product. It only has three directions: horizontal, vertical and diagonal. It is optimal in representing point singularity, but it is not optimal for the representation of two-dimensional information such as edge, contour and curve in the image, resulting in a large number of invalid decomposition. In recent years, new multiscale geometric analysis tools have been proposed to solve two-dimensional or higher anisotropy. Ridgelet [10], curvelet [11], Contourlet [12] have been successfully applied in some aspects of image processing.

Contourlet transform is an image analysis method based on geometric features, which can decompose the image in multiple scales and directions, and is suitable for the analysis of line singular features. However, because it contains down sampling process, it does not have translation invariance, resulting in pseudo Gibbs effect and image distortion. To solve this problem, reference [13] proposed a non-sampled Contourlet transform (NSCT) with translation invariance. NSCT retains the excellent characteristics of CT: it meets the anisotropic scale relationship and has good directivity. It can accurately capture the edge contour information and texture detail information in the image. It is suitable for expressing multi-sensor images with rich detail and direction information. After NSCT decomposition, multi-sensor images will eventually produce a low-frequency subband and multiple high-frequency directional subbands. In the past, most of the algorithms based on regional energy are used to represent the importance of the decomposed coefficients of the source image, and the fusion rules are established. However, the different imaging mechanisms of sensors lead to great differences in the obtained images. The fusion method using the same regional energy does not make full use of its imaging characteristics and image information characteristics.

References [14] and [15] proposed a neural network based on pulse coupling (pulse coupled neural network, PCNN, PCNN is a new type of neural network different from the traditional artificial neural network, with the characteristics of synchronous excitation and variable threshold. The image fusion method based on PCNN is a global image fusion method, which can retain more detailed information and achieve better fusion effect when applied to the field of image fusion. Reference [16] The Laplace energy of image blocks is used as the input stimulus of each neuron in PCNN; literature [17] takes the contrast pyramid decomposition coefficient as the input stimulus of each neuron in PCNN to realize the image fusion research based on PCNN; literature [18] realizes the pixel level image fusion based on PCNN model by defining the pixel by

pixel definition of the image as the link strength of the corresponding neurons in PCNN; literature [18] [19] Using the fusion method of lifting wavelet transform and PCNN, the link strength of all neurons is selected the same value according to experiment or experience

In this paper, an NSCT image fusion algorithm combining PCNN and golden section method is proposed. Firstly, NSCT is used to decompose the image for multi-scale decomposition to obtain the depth feature information in the image. In the high-frequency subband, PCNN is used to design the fusion strategy and improve the fusion performance. In the low-frequency subband, the traditional weighted summation method is abandoned and the golden section method is adopted [20] Search the optimal low-frequency fusion weight and adaptively fuse the low-frequency subband coefficients of multi-sensor images. Experiments show that this fusion algorithm is applied to the fusion of ordinary images and medical images, and good fusion results are obtained by comparing with other algorithms.

## 2. NSCT Image Fusion Algorithm Combining PCNN and Golden Section Method

### 2.1 Basic Principle of NSCT

The construction of NSCT is based on non-sampled tower decomposition (NSP) and non-sampled directional filter bank (NSDFB). The two parts are independent of each other, as shown in Fig. 1 (a). NSP provides multi-scale decomposition and NSDFB provides multi-directional decomposition. Firstly, NSP decomposes the input image into scales. At each scale, DFB decomposes the decomposed bandpass signal into several directional subbands, and the number of directional subbands can be any power of 2 (Fig. 1 (b)). This process can be repeated in the low-frequency subband of NSP output.

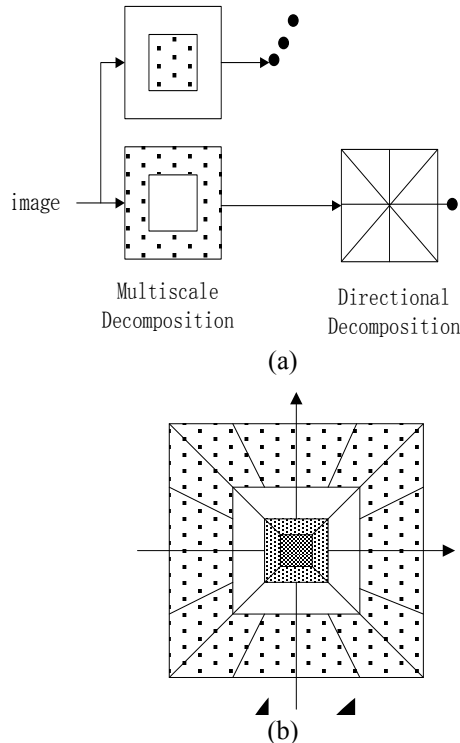


Fig. 1 (a). NSCT block decomposition diagram  
(b) NSCT frequency division diagram

NSP is constructed by a two channel non-sampling filter bank. There are no up sampling and down sampling steps, so it is translation invariant. After NSP decomposes the image into various scales, NSDFB can divide an image into arbitrary power directions of 2 on each scale, and meet the translation invariance. NSCT is redundant. The redundancy of NSCT is  $W = \sum_{i=0}^{l-1} 2^{d_i}$ , where  $2^{d_i}$  is the number of high-frequency subbands on scale  $2^{-i}$ .

### 2.2 PCNN Model

PCNN is a new type of neural network different from the traditional artificial neural network. It is a feedback network composed of several neurons interconnected. Each neuron is composed of three parts: receiving part, modulation part and pulse generation part (as shown in Fig. 2).

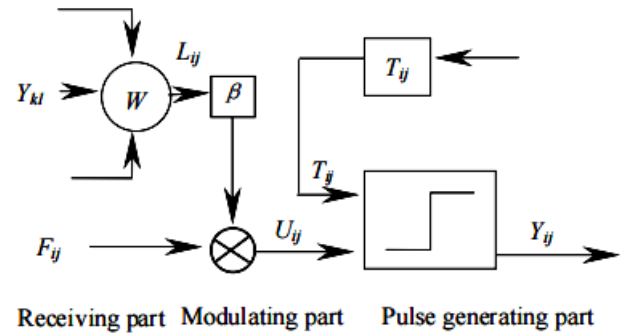


Fig.2. Single neural cell model

When PCNN is used for  $M \times N$  image processing, the gray value of each pixel must be used as the input of each neuron. Therefore, the  $M \times N$  image matrix corresponds to the neural network composed of  $M \times N$  PCNN neurons, and the activity of  $N_{ij}$  of each neuron can be described by the following formula:

$$F_{ij}[n] = e^{-\alpha_F} F_{ij}[n-1] + S_{ij} + V_F \sum_k M_{ijk} Y_{kl}[n-1] \quad (1)$$

$$L_{ij}[n] = e^{-\alpha_L} L_{ij}[n-1] + V_L \sum_k M_{ijk} Y_{kl}[n-1] \quad (2)$$

$$L_y[n] = e^{-\alpha_L} L_y[n-1] + V_L \sum_k M_{ijk} Y_{kl}^1[n-1] + V_N \sum_k M_{ijk} Y_{kl}^2[n-1] \quad (3)$$

$$U_{ij}[n] = F_{ij}[n](1 + \beta L_{ij}[n]) \quad (4)$$

$$T_{ij}[n] = e^{-\alpha_T} T_{ij}[n-1] + V_T Y_{ij}[n] \quad (5)$$

$$Y_{ij}[n] = \begin{cases} 1 & U_{ij}[n] \geq T_{ij}[n] \\ 0 & \text{otherwise} \end{cases} \quad (6)$$

Where:  $S_{ij}$ ,  $U_{ij}$ , and  $Y_{ij}$  are the external stimulation (input), internal behavior, and output of neuron  $N_{ij}$ , respectively;  $L_{ij}$  and  $F_{ij}$  are the two input channels of link domain and feedback domain respectively,  $m$  and  $W$  are the connection weight coefficient matrix between neurons,  $V_F$  and  $V_L$  ( $V_N$ ) are the amplification coefficients of feedback domain and link domain respectively;  $T_{ij}$ , and  $V_T$  are variable threshold function output and threshold amplification factor,  $\alpha_L$ ,  $\alpha_F$  and  $\alpha_T$  is the time constant of link domain, feedback domain and variable threshold function respectively.

The unique neuron capture characteristic of PCNN model - the ignition of a neuron will cause the capture and ignition of adjacent neurons with similar brightness to the neuron, which can automatically realize information transmission and information coupling. Therefore, this unique characteristic of PCNN lays a foundation for the application of PCNN in image

fusion. In order to better apply PCNN algorithm to image fusion, we use double-layer parallel PCNN model. In this model, any one of the two registered images to be fused is used as the neuron of the master PCNN and the other as the neuron of the slave PCNN. The activity equation of the master neuron is calculated by equations (1), (3) ~ (6), and the activity equation of the slave neuron is calculated by equations (1), (2) and (4) ~ (6). With the help of the capture characteristics of PCNN, the double-layer parallel PCNN network can input the ignition information of the slave PCNN neuron into the link domain of the corresponding neuron of the main PCNN, so as to fuse the neuron information in the slave PCNN with the corresponding neuron information of the main PCNN. That is, after setting the master and slave neurons to ignite a neuron in the slave PCNN, the ignition information is not only transmitted to the connected neurons, but also to the corresponding neurons of the master PCNN, so as to realize image fusion.

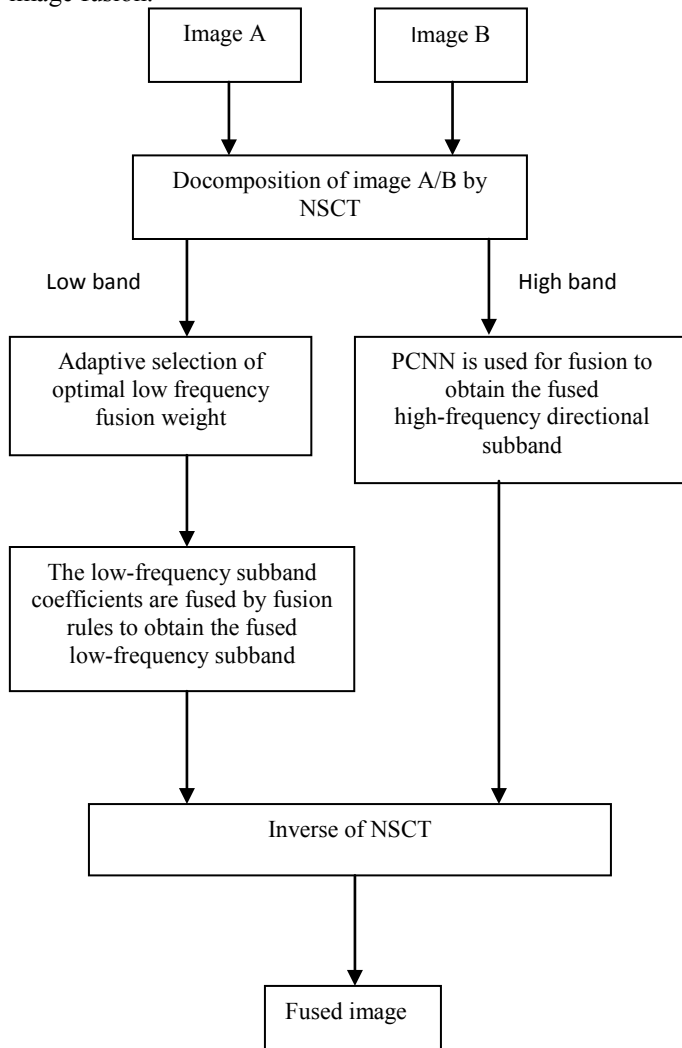


Fig.3. Implementation of image fusion algorithm based on NSCT

### 2.3 Implementation of Fusion Algorithm

In the process of image fusion, the selection of fusion rules is very important for the quality of fusion. Based on NSCT multi-scale decomposition, PCNN and golden section are used

to fuse the high and low frequency components of the image. Considering that the low-frequency subbands of NSCT are positive coefficients and contain most of the energy information of the image, the following formula is generally used to obtain the transformation coefficient of the low-frequency subband of the fused image,  $w$  is the fusion weight, and the low-frequency subband fusion rule is:

$$S_L^F(n, m) = w * S_L^A(n, m) + (1 - w) * S_L^B(n, m) \quad w \in [0, 1] \quad (7)$$

The low-frequency subband fusion weight is the optimal search using the golden section method to adaptively fuse the low-frequency subband coefficients of multi-sensor images. The golden section method shortens the search interval by removing the interval other than the "bad point" and leaving the interval where the "good point" is located. After repeatedly comparing the function value at the trial point, the position of the optimal weight can be estimated more and more accurately. The objective function is taken as the edge fusion quality index that can reflect the edge preservation of the fused image  $Q_E(w)$ . The higher the value of this index, the better the quality of the fused image.

The following takes the fusion of two images as an example to illustrate the implementation of image fusion algorithm based on non-sampling Contourlet transform. The fusion process is shown in Fig.3.

The source images A and B are decomposed by layer NSCT respectively. Firstly, the image is decomposed by non-sampling tower decomposition to obtain the low-frequency subband  $S_l$  and passband  $D_l$  on each scale, that is  $\{S_l^A(n, m), 0 \leq l \leq L-1\}, \{S_l^B(n, m), 0 \leq l \leq L-1\}$ , the low-frequency subband is and the passband is  $\{D_l^A(n, m), 0 \leq l \leq L-1\}, \{D_l^B(n, m), 0 \leq l \leq L-1\}$ . Then, the non-sampling filter bank NSDFB decomposes the passband into a plurality of wedge-shaped high-frequency directional subbands  $\{D_{l,i}^A(n, m), 0 \leq l \leq L-1, 1 \leq i \leq k_l\}, \{D_{l,i}^B(n, m), 0 \leq l \leq L-1, 1 \leq i \leq k_l\}$ ,  $k_l$  represents the number of high-frequency directional subbands of the image on scale  $2^{-l}$ , and  $D_{l,i}^A(n, m)$  represents the  $i$ th directional subband of image a on scale  $2^{-l}$ . The specific fusion steps are as follows:

Step1: for  $S_l^A(n, m)$  and  $S_l^B(n, m)$ , The golden section method is used to adaptively search the optimal low-frequency subband fusion weight  $w^*$ ;

Step2: The low-frequency subband coefficients of multi-sensor source images are fused by using the searched optimal low-frequency subband fusion weight  $w^*$  and low-frequency fusion rules (equation (8)). The objective function is taken as the edge fusion quality index  $Q_E$ . Represented by T, let the initial value of the interval to be searched  $[a, b]$  be  $[0, 1]$ , the minimum length  $\varepsilon = 0.01$  of the interval to be searched, and the specific implementation steps of the optimal fusion weight  $w^*$  adaptive search algorithm are as follows:

- 1) Trial points  $w_1$  and  $w_2$  for calculating the fusion weights of low frequency subbands in the initial search interval  $[a, b]$ ,  $w_1 = a + 0.382 * (b - a)$ ,  $w_2 = a + b - w_1$ ,  $w_1, w_2 \in [a, b]$ ;
- 2) Calculate the objective function value  $T(w_1)$  of the trial point  $w_1$ ;
- 3) Calculate the objective function value  $T(w_2)$  of the trial point  $w_2$ ;
- 4) if  $T(w_1) > T(w_2)$ , then update  $a = w_1$ , and go to step 5) ; Otherwise go to step 6) ;
- 5) if  $|b - a| < \varepsilon$ , the  $w^* = (a + b) / 2$ , stop searching; Otherwise update  $w_1$  and  $w_2$ .  $w_1 = w_2$ ,  $w_2 = a + 0.618 * (b - a)$ , go to step 2) ;
- 6) update  $b = w_2$ ;
- 7) if  $|b - a| < \varepsilon$ , 则  $w^* = (a + b) / 2$ , stop searching; Otherwise update  $w_1$  and  $w_2$ :  $w_2 = w_1$ ,  $w_1 = a + 0.382 * (b - a)$ , go to step 2) ;

Step3: For high-frequency directional subbands on various scales of multi-sensor source images, choose  $D_{l,i}^A(n, m)$  as the input of master PCNN,  $D_{l,i}^B(n, m)$  as the input of slave PCNN. And set the initial value of PCNN parameters;

Step4: For each iteration of the master-slave PCNN network:

- 1) Calculate each neuron of the slave PCNN model according to formula (1), (2), (4) and (6), feed back the output of the slave PCNN neuron to the link domain of the corresponding master PCNN neuron, and calculate the network output value of PCNN according to formula (1), (3) ~ formula (6);
- 2) A series of multi-scale fusion images output from PCNN network are reconstructed, and the final reconstructed image is the fusion result of this iteration;
- 3) The information entropy of the fused image is calculated according to the following formula.

$$H = - \sum_{i=0}^{L-1} p_i \log p_i \quad (8)$$

Where,  $H$  represents the entropy of the image,  $L$  represents the total gray level of the image, and  $p_i$  represents the sum of the number of pixels with gray value and the total number of pixels of the image, and  $p_i = N_i / N$ . Image information entropy is an important index to measure the richness of image information. Through the comparison of image information entropy, the detail performance ability of image can be compared. The size of entropy reflects the amount of information carried by the image. The larger the entropy of the fused image, the greater the amount of information the fused image carries.

Step5: take the maximum information entropy of the output image of the parallel PCNN network as the final fusion result of the high-frequency subband.

Step6: perform NSCT inverse transform on the low-frequency subband and high-frequency direction subband of the fused image to obtain the fused image  $F$ .

### 3. Experimental Results and Analysis

The objective evaluation of the fused image [21-22] should conform to the subjective evaluation, comprehensively considering the richness of image information and the maintenance of spatial edge detail information of the source image.

#### 3.1 Image Fusion Evaluation Index

The evaluation indexes adopted in this paper are:

(1) Mutual information: an important concept in information theory, which can be used to measure the correlation between two variables. Therefore, mutual information can be used to measure the correlation between the fused image and the source image to evaluate the fusion effect. The larger the value, the more information the fused image obtains from the source image, and the better the fusion effect. The mutual information between the fused image and the source images A and B is expressed as:

$$I_{FB} = \sum_{k=0}^{L-1} \sum_{j=0}^{L-1} P_{FB}(k, j) \log 2 \frac{P_{FB}(k, j)}{P_F(k)P_B(j)} \quad (9)$$

$$I_{FB} = \sum_{k=0}^{L-1} \sum_{j=0}^{L-1} P_{FB}(k, j) \log 2 \frac{P_{FB}(k, j)}{P_F(k)P_B(j)} \quad (10)$$

Where  $P_A, P_B$  and  $P_F$  are the probability densities of images A, B and F, and  $P_{FA}(k, i)$  and  $P_{FB}(k, i)$  are the joint probability densities of the fused image and the source image, respectively. In this paper, the total information of the fused image including the source image is taken as the total mutual information, and then divided by the sum of the information entropy of the source image, which is normalized to  $[0, 1]$ , that is:

$$MI = \frac{I_{FA} + I_{FB}}{H_A + H_B} \quad (11)$$

Edge-dependent fusion quality index(EFQI). EFQI is a new objective index proposed in recent years to evaluate the quality of fused image, which can reflect the edge preservation of fused image and the strength of ringing effect around the edge. It is defined as:

$$Q_E(A, B, F) = Q_w(A, B, F)^{1-\alpha} \cdot Q_w(A', B', F)^\alpha \quad (12)$$

Where  $Q_E$  represents EFQI and  $Q_w$  is the weighted fusion evaluation index.  $A', B'$  and  $F'$  are edge images of source images A, B and fused image  $F$ , respectively. Parameter  $\alpha \in [0, 1]$  reflects the importance of the edge image in the original image. The closer  $\alpha$  is to 1, the more important the edge image is. The larger the EFQI, the higher the quality of the fused image.

#### 3.4' Cpcr[ukr]qhl'eqo r c t c v l x g' l z r g t k o g p w i t g u m m u'

The images in the experiment are decomposed by four layers. In the wavelet based fusion strategy, when selecting the wavelet basis function, we should consider the problem that the fusion result may produce artificial effects on vision, especially ringing and jitter. This is related to the discrete characteristics of sampling when down sampling is applied. If a non integer

number of signals is shifted and there is a constant local area connected to the sharp edge, the ringing will be enhanced. After interpolation, translation and resampling, the new sampling cannot be expressed as a constant in the transform domain, but tends to oscillate (Gibbs phenomenon). In the wavelet based fusion strategy, short decomposition or reconstruction filters should be used to avoid ringing. However, a very short filter will make the frequency selectivity worse. Considering comprehensively, Daubechies filter with 8 or 10 coefficients can provide better execution results for multi-scale image fusion. The wavelet basis selected in WTF and SWTF is 'db8'. Both CT and NSCT adopt the classical '9-7' tower decomposition and 'C-D' direction filter bank. The decomposition number of subbands from fine scale to coarse scale is 16, 8, 4 and 4. The fusion rule used in the multi-scale image fusion method as a comparison in the experiment is: the approximate approximation coefficient at the minimum scale takes the mean value, and the decomposition coefficient with the largest absolute value is selected as the decomposition coefficient of the fused image.

The images in the experiment are decomposed by four layers. In the wavelet based fusion strategy, when selecting the wavelet basis function, we should consider the problem that the fusion result may produce artificial effects on vision, especially ringing and jitter. This is related to the discrete characteristics of sampling when down sampling is applied. If a non integer number of signals is shifted and there is a constant local area connected to the sharp edge, the ringing will be enhanced. After interpolation, translation and resampling, the new sampling can not be expressed as a constant in the transform domain, but tends to oscillate (Gibbs phenomenon). In the wavelet based fusion strategy, short decomposition or reconstruction filters should be used to avoid ringing. However, a very short filter will make the frequency selectivity worse. Considering comprehensively, Daubechies filter with 8 or 10 coefficients can

provide better execution results for multi-scale image fusion. The wavelet basis selected in WT is 'db8'. NSCT adopts the classical '9-7' tower decomposition and 'C-D' direction filter bank. The decomposition number of subbands from fine scale to coarse scale is 16, 8, 4 and 4. The fusion rule used in the multi-scale image fusion method as a comparison in the experiment is: the approximate approximation coefficient at the minimum scale takes the mean value, and the decomposition coefficient with the largest absolute value is selected as the decomposition coefficient of the fused image.

Table 1 shows the comparison of several metrics of fusion results of several algorithms. IM1 ~ IM4 are the change curve of objective function and the change curve of information entropy[16] and mutual information[17] of fused image obtained by using corresponding weight W. By observing the experimental data in Table 1, it can be found that NSCT has certain advantages in information entropy, mutual information and edge fusion quality.

The fusion effects of image fusion based on WT and NSCT are shown in Figure 2. It can be found from the figure that the fused image of this algorithm not only retains the direction texture information of the image, but also effectively eliminates the edge "burr" effect, the edge is clear and the ghosting is eliminated. This is because NSCT fully captures the texture information in different directions, gives a sparse representation of the high anisotropy in the image, and the local energy operator fully maintains the local direction characteristics, The details are well preserved and good image fusion effect is obtained, which is better than NSCT fusion method.

Table 1 shows the comparison of several metrics of the fusion results of various algorithms. Observing the experimental data in Table 1, it can be found that the algorithm in this paper has certain advantages in information entropy, mutual information and edge fusion quality. In terms of visual effect, as shown in

**TABLE I.** Comparison of experimental result

Images	Fused method				
	Criteria	WTF	SWTF	CTF	Proposed
Clock <sup>A/B</sup>	MI	6.6299	7.1007	7.4105	8.4101
	$Q^{AB/F}$	0.6789	0.7211	0.7298	0.7521
Baboon <sup>A/B</sup>	MI	5.5965	6.1906	6.3610	7.5002
	$Q^{AB/F}$	0.5701	0.6114	0.6418	0.7124
Hat <sup>A/B</sup>	MI	6.9603	7.0109	7.4201	7.6017
	$Q^{AB/F}$	0.6659	0.6941	0.7802	0.8121
CT&MIR <sup>A/B</sup>	MI	3.1006	4.0247	4.2099	4.3640
	$Q^{AB/F}$	0.6174	0.6429	0.6802	0.7461

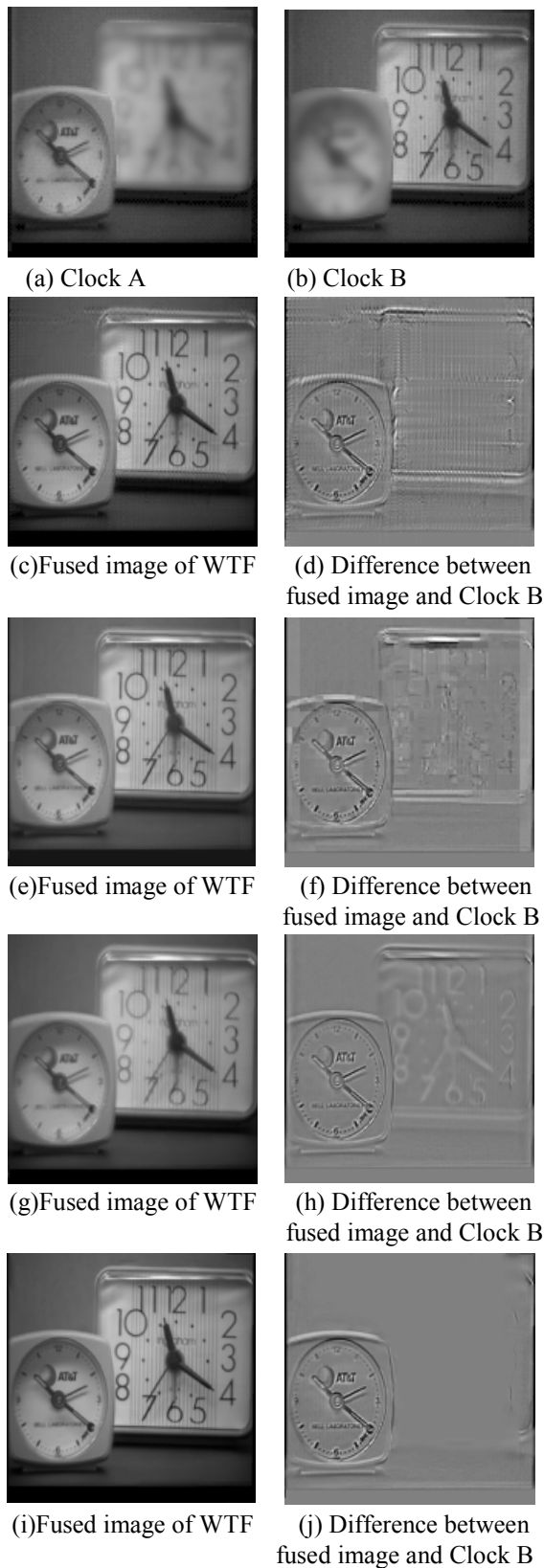


Fig.4. Image fusion results of ClockA/B

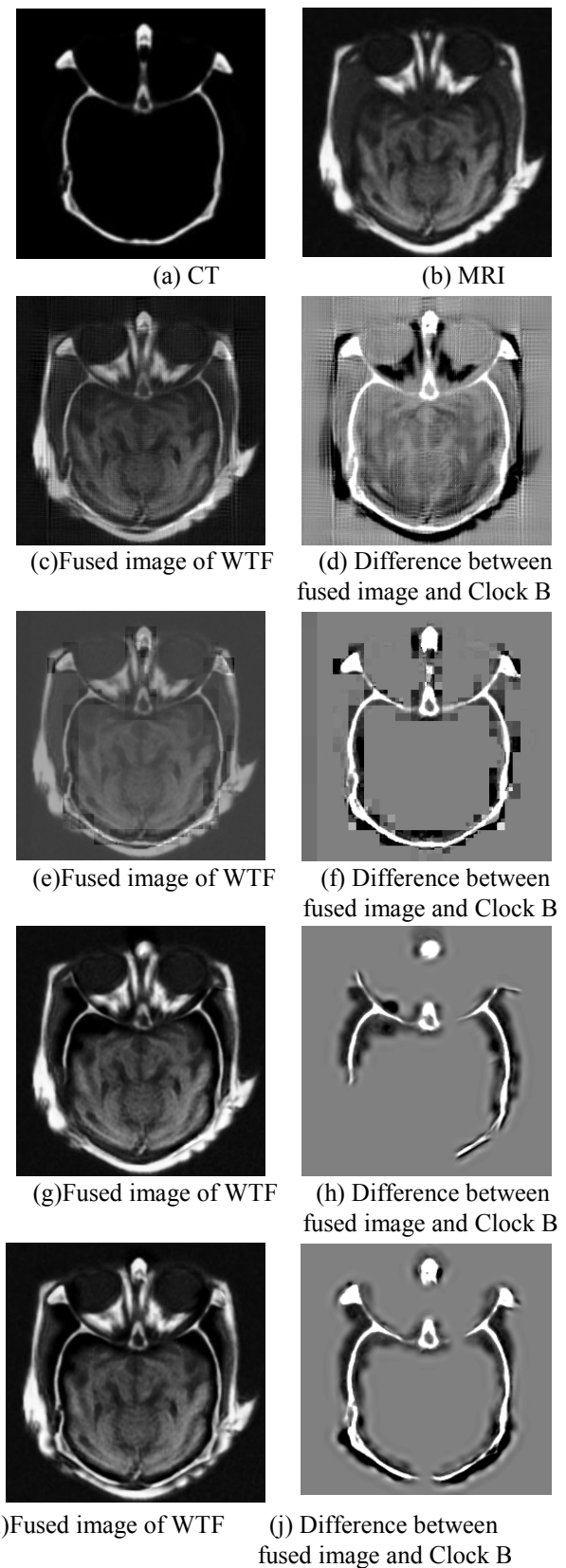


Fig. 5. Image fusion results of Clock A/B

Fig.4.and Fig.5., there is a ringing phenomenon in WTF, which is caused by the fact that WTF is not a non- sampling transformation. The fusion effect of SWTF and CTF is not ideal, because they do not fully consider the difference between coefficients. Whether in the fused image or difference image,

the algorithm can effectively find the focused part of the source image, and the fused image appears smooth and clear in these

## 4. Conclusions

Because the non-sampled Contourlet has translation invariance, it can effectively avoid the image distortion caused by the lack of translation invariance of some transformations. Moreover, Contourlet can also effectively capture the multi-scale and multi-directional information in the image, which is very suitable for expressing multi-sensor images with rich direction and fine texture information. In this paper, non-sampling Contourlet is applied to the field of multi-sensor image fusion, and a multi-sensor image adaptive fusion method based on non-sampling Contourlet is proposed. For high-frequency images, PCNN fusion rules are adopted. For low-frequency components, multi-sensor images can adaptively select the best low-frequency fusion weight and make full use of image information. Experimental results show that this method can obtain clear and detailed fusion images of target scene, and is an effective and feasible fusion method.

## References

- [1] James A P, Dasarathy B V. Medical image fusion: A survey of the state of the art[J]. *Information fusion*, **2014**, 19: 4-19.
- [2] Jinju J, Santhi N, Ramar K, et al. Spatial frequency discrete wavelet transform image fusion technique for remote sensing applications[J]. *Engineering Science and Technology, an International Journal*, **2019**, 22(3): 715-726.
- [3] Ghassemian H. A review of remote sensing image fusion methods[J]. *Information Fusion*, **2016**, 32: 75-89.
- [4] Ma J, Ma Y, Li C. Infrared and visible image fusion methods and applications: A survey[J]. *Information Fusion*, **2019**, 45: 153-178.
- [5] Liu Y, Chen X, Wang Z, et al. Deep learning for pixel-level image fusion: Recent advances and future prospects[J]. *Information Fusion*, **2018**, 42: 158-173.
- [6] Bhavana V, Krishnappa H K. Multi-modality medical image fusion using discrete wavelet transform[J]. *Procedia Computer Science*, **2015**, 70: 625-631.
- [7] Yang Y, Huang S, Gao J, et al. Multi-focus image fusion using an effective discrete wavelet transform based algorithm[J]. *Measurement science review*, **2014**, 14(2): 102.
- [8] Mehra I, Nishchal N K. Image fusion using wavelet transform and its application to asymmetric cryptosystem and hiding[J]. *Optics express*, **2014**, 22(5): 5474-5482.
- [9] Singh D, Garg D, Singh Pannu H. Efficient landsat image fusion using fuzzy and stationary discrete wavelet transform[J]. *The Imaging Science Journal*, **2017**, 65(2): 108-114.
- [10] Do M N, Vetterli M. The finite ridgelet transform for image representation[J]. *IEEE Transactions on image Processing*, **2003**, 12(1): 16-28.
- [11] Ma J, Plonka G. The curvelet transform[J]. *IEEE signal processing magazine*, **2010**, 27(2): 118-133.
- [12] Do M N, Vetterli M. The Contourlet transform: an efficient directional multiresolution image representation[J]. *IEEE Transactions on image processing*, **2005**, 14(12): 2091-2106.
- [13] Xiang T, Yan L, Gao R. A fusion algorithm for infrared and visible images based on adaptive dual-channel unit-linking PCNN in NSCT domain[J]. *Infrared Physics & Technology*, **2015**, 69: 53-61.
- [14] Ding S, Zhao X, Xu H, et al. NSCT-PCNN image fusion based on image gradient motivation[J]. *IET Computer Vision*, **2018**, 12(4): 377-383.
- [15] Zhang S, Liu B, Huang F. Multimodel fusion method via sparse representation at pixel-level and feature-level[J]. *Optical Engineering*, **2019**, 58(6): 063105.
- [16] Huang W, Jing Z L. Multi-focus image fusion using pulse coupled neural network [J]. *Pattern Recognition letters*, **2007**, 28(9): 1123-1132.
- [17] Xu BC, Chen Z. A multisensor image fusion algorithm based on PCNN[C] // *Proceedings of the 5th World Congress on Intelligent Control and Automation*. Hangzhou: Institute of Electrical and Electronics Engineers Inc, **2004**: 3679-3682.
- [18] Miao Qiguang, Wang Baoshu. A novel algorithm of multi-focus image fusion using adaptive PCNN [J]. *Journal of Electronics & Information Technology*, **2006**, 28(3): 466-470.
- [19] Chen Hao. Study on multi-source image fusion based on multi-scale transform[D]. Beijing: Graduate University of Chinese Academy of Sciences, **2010**.
- [20] Chen Kaizhou. Optimization calculation method, Northwest Institute of Telecommunication Engineering Press[D], **1986**.
- [21] Bai Q, Jin C. "Image Fusion And Recognition Based On Compressed Sensing Theory". *International Journal on Smart Sensing & Intelligent Systems*, Vol. 8, No. 1, **2015**.
- [22] Petrovic V, Xydeas C. "On the effects of sensor noise in pixel-level image fusion performance"[C]. In: *Proceedings of the 3rd International Conference on Image Fusion*. Paris, France: IEEE, **2000**, pp. 14-19.

Pai Zhang (M'02–SM'06–F'09) received the B.S. and the M.S. degree in School of information engineering from Yanshan University, China, in 2006 and 2009 respectively, Ph.D. degrees in School of electrical engineering from the Yanshan University, Qinhuangdao, China, in 2013. From 2013 to now, she worked at College of Intelligence and Information Engineering Tangshan College, China. Her current research interest is in the area of multiscale signal processing and applications in image analysis.

## Creative Commons Attribution License 4.0 (Attribution 4.0 International, CC BY 4.0)

This article is published under the terms of the Creative Commons Attribution License 4.0  
[https://creativecommons.org/licenses/by/4.0/deed.en\\_US](https://creativecommons.org/licenses/by/4.0/deed.en_US)